Article

Tuning Crystal Structures of Iron-Based Metal−Organic Frameworks for Drug Delivery Applications

Hao Pham, Kimberly Ramos, Andy Sua, Jessica Acuna, Katarzyna Slowinska, Travis Nguyen, Angela Bui, Mark D. R. Weber, and Fangyuan Tian*

Cite This: *ACS Omega* 2020, 5, 3418−3427

Read Online

ACCESS | Metrics & More | Article Recommendations | Supporting Information

ABSTRACT: Iron-based metal−organic frameworks (Fe-MOFs) have emerged as promising candidates for drug delivery applications due to their low toxicity, structural flexibility, and safe biodegradation in a physiological environment. Here, we studied two types of Fe-MOFs: MIL-53 and MIL-88B, for in vitro drug loading and releasing of ibuprofen as a model drug. Both Fe-MOFs are based on the same iron clusters and organic ligands but form different crystal structures as a result of two different nucleation pathways. The MIL-53 structure demonstrates one-dimensional channels, while MIL-88B exhibits a three-dimensional cage structure. Our studies show that MIL-53 adsorbs more ibuprofen (37.0 wt %) compared to MIL-88B (19.5 wt %). A controlled drug release was observed in both materials with a slower elution pattern in the case of the ibuprofen-encapsulated MIL-88B. This indicates that a complex cage structure of MIL-88 is beneficial to control the rate of drug release. A linear correlation was found between cumulative drug release and the degree of material degradation, suggesting the biodegradation of Fe-MILs as the main drug elution mechanism. The cytotoxicity of MIL-88B was evaluated in vitro with NIH-3T3 Swiss mouse fibroblasts, and it shows that MIL-88B has no adverse effects on cell viability up to 0.1 mg/mL. This low toxicity was attributed to the morphology of MIL-88B nanocrystals. The very low toxicity and controlled drug release behavior of Fe-MIL-88B suggest that better materials for drug-delivery applications can be created by controlling not only the composition but also the crystal structure and nanoparticle morphology of the material.
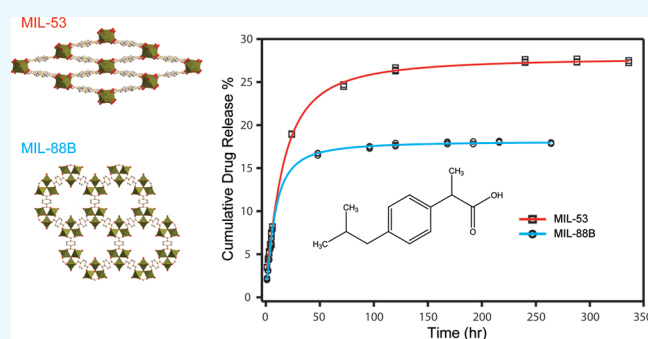
1. INTRODUCTION

The rapid growth of drug discovery and the increasing demand for drug-eluting medical implants accelerate the search for new drug carrier systems with low toxicity, better control of drug loading capacity, and sustainable drug releasing. So far, polymeric and inorganic complexes have been widely applied for the drug delivery and controllable release of pharmaceutical compounds. In particular, poly(lactic-*co*-glycolic acid) (PLGA), polymers and their polymeric particles have been used in a variety of therapeutic devices due to their excellent biocompatibility.[1−3] The inorganic solids, such as porous silicon, functionalized silica, and zeolites, are also utilized as drug carriers.[4−6] Some of these organic and inorganic materials have limited drug loading capacity and complex interactions of loaded drugs at the guest−host interface. As an alternative, a type of hybrid materials, metal−organic frameworks (MOFs), combining the advantages of polymers and inorganic mesoporous solids, have emerged as drug delivery matrices.[7−11]

MOFs are solid porous crystals composing of metal ions or clusters as secondary building blocks (SBUs) cross-linked by organic ligands.[12,13] Due to the high porosity, large surface area, and suitable pore sizes, MOFs have exhibited potential in many applications, such as gas separation and storage, catalysis, and loading other guest molecules.[14−18] More recently, increasing interest has been attracted to apply MOFs for biomedical applications, such as imaging, sensing, and loading therapeutic agents as delivery vehicles.[19−21] Compared to other traditional drug carriers (i.e., polymers, nanoparticles, bacteria, etc.), MOFs exhibit an excellent drug loading capacity and controlled release profile of many therapeutic agents, attributed to their porous structures.[19,22] In addition, MOFs can be engineered for specific drug delivery due to the flexibility and versatile chemical composition of the framework. For example, a rigid MOF, MIL-100 (MIL stands for Material Institut Lavoisier), is able to hold up to 21.2 wt % azidothymidine triphosphate (AZT-TP, an antiretroviral drug for HIV/AIDS treatment), while its loading capacity can be

increased to 42.0 wt % when amino-functionalized MIL-100 is used.[9] In comparison, traditional drug carriers have a much lower loading capacity (i.e., polymer nanoparticles, ~6 wt %; liposomal systems, <1 wt %).[23,24] Despite the MOFs advantage of high drug loading and effective delivery, an ongoing issue of its safety and biocompatibility is questioned. In the last five years, many studies have been conducted to test cytotoxicity of MOFs with various cell and animal models.[25,26] One type of MOF, iron-containing MOFs (Fe-MOFs), has truly stood out for their supreme safety and biodegradability.[11,22,27] A majority of Fe-MOFs belong to the MIL and BioMOF families, including MIL-53, MIL-88, MIL-100, MIL-101, BioMOF-1, and BioMOF-5.[10,19,28−31] Selection of a drug delivery system is based on drug formulation, delivery routes, targeting organs/cells, etc. Therefore, it is crucial to select the correct MOF for a particular drug and for a specific target. So far, little research has been done to optimize MOF structures for a certain delivery route. In addition, other factors should also be considered, such as the guest−host interaction, pore size, cavity volume, and stability, especially when a MOF is paired with a therapeutic agent. Most MOFs contain hydrophobic properties due to their organic ligands, making them efficient in adsorbing hydrocolloids and lipophilic drugs. However, most MOFs lack stability in aqueous conditions due to their relatively weak coordination bonding between metal clusters and ligands. The degradation of MOFs in aqueous solutions can be viewed as an advantage when considering a potential biodegradable drug delivery system. Structural decomposition provides an easy method for releasing encapsulated drug molecules; however, the kinetics of decomposition and retention of MOF structure in a biological environment is not well understood. Additionally, when designing MOFs for drug delivery, it is important to take into consideration their wettability and stability.

In this study, we focused on using unstable Fe-MOFs as biodegradable drug delivery systems. This work aims at studying two aspects of Fe-MOFs: (A) the effect of crystal structure on drug loading/adsorption and (B) the interactions between the guest molecules and host matrix (drug and MOFs), including drug elution kinetics and material degradation.

Fe-based MIL-53 and MIL-88B are two flexible Fe-MOFs consisting of iron ligands connected by terephthalate (TA) linkers. It has been found that MIL-53 forms through a homogenous nucleation and MIL-88B through a heterogeneous nucleation.[32] MIL-53 consists of oxygen-centered iron-carboxylate trimers (octahedral shaped FeO_6) connected by TA linkers forming rhomb-shaped 1D channels.[33] Composing of the same FeO_6 clusters and TA ligands, MIL-88B exhibits a hexagonal 3D structure.[30] Here, we show that differences in crystal structure results in various characteristics in drug (ibuprofen) loading and delivery. Ibuprofen was selected as the model drug in this study due to its structural simplicity and size. Powder X-ray diffraction (PXRD), infrared spectroscopic studies, and nitrogen sorption isotherms have been performed to determine the drug adsorption and interface interactions within the carriers' systems. Various kinetic models were used to evaluate the drug release profiles of MIL-53 and MIL-88B. The biocompatibility was tested in vitro with NIH-3T3 Swiss mouse fibroblasts. We believe that the joint effort of MIL synthesis coupled with cell model studies will provide a deep and systematic understanding of these two Fe-based MIL materials as drug delivery systems. Additionally, we focused on

the role of the crystal structure toward drug delivery by illustrating three drug elution models that can be applied to other MOFs.

2. RESULTS AND DISCUSSION

2.1. Characterization of Materials and Drug Loading Studies. MIL-88B and MIL-53 contain the same ligands, but their formation is guided by different nucleation processes that can be controlled by different synthetic conditions. The crystal structures of MIL-88B and MIL-53 before and after loading with ibuprofen were studied using powder X-ray diffraction (PXRD). As shown in Figure 1a, the PXRD patterns of MIL-
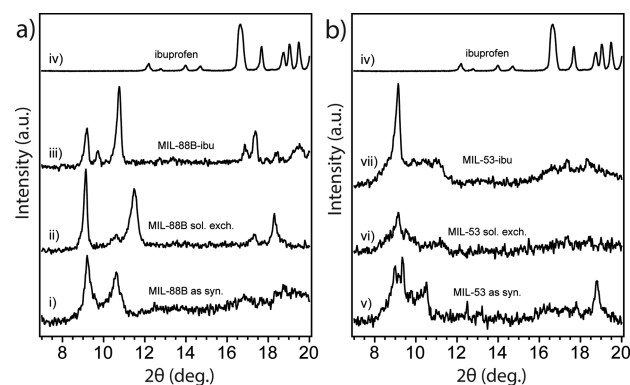

Figure 1. PXRD patterns of (a) MIL-88B and (b) MIL-53 at the condition of (i) as-synthesized, (ii) after solvent exchange, and (iii) after loading with ibuprofen, in comparison to the PXRD patterns of (iv) pure ibuprofen.

88B are in good agreement with previous studies.[39,40] MIL-88B exhibited three characteristic diffraction peaks at 9.14°, 10.60°, and 11.48° representing the 002, 100, and 101 phases, respectively.[10] We noticed that the diffraction feature was shifted from 10.62° for as-synthesis MIL-88B to 11.48° for the same bulk crystal after solvent exchange followed by further thermal activation. A diffraction angle shifting to a larger angle indicates the shrinkage of the crystal cell based on the Bragg's Law,[41] This increase in the angle confirms the decreased cage volume of MIL-88B once the trapped DMF solvent inside crystals was replaced and removed. Moreover, after loading with ibuprofen, the MIL-88B pore volume was expanded reflected by the decrease in diffraction angle for the same 101 peak. Our results confirmed the structural flexibility of both MIL-53 and MIL-88B as the "breathing effect" enables both materials to trap guest molecules with shrinkable frameworks, which is consistent with previous literature.[28,42−44] Figure 1b shows the PXRD patterns for MIL-53 as synthesized, after solvent exchange, and loaded with ibuprofen. The diffraction angle at 9.1° is a significant feature for MIL-53.[45,46] After loading with ibuprofen, both MIL-53 and MIL-88B exhibited crystal structures from both host and guest materials. Extra PXRD features at 16.6° and 19.4° were observed on both MILs after loading with ibuprofen, indicating that ibuprofen was added to both porous solids.[47] It is critically important to determine the location of guest drug molecules relative to the host material; therefore, we further performed gas sorption studies to study the porosity changes corresponding to drug loading in the next part. The chemical compositions of both MILs are identical as confirmed by our attenuated total reflectance infrared (ATR-IR) studies, shown in Figure 2. Both
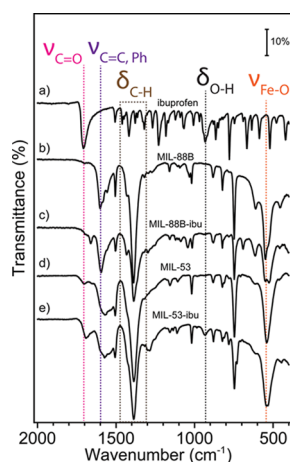
Figure 2. ATR-IR spectra of (a) pure ibuprofen, (b) pristine Fe-MIL-88B, (c) ibuprofen loaded Fe-MIL-88B, (d) pristine Fe-MIL-53, and (e) ibuprofen loaded Fe-MIL-53.

Figure 3. N_2 sorption isotherms of Fe-MIL-88B (black) and Fe-MIL-53 (red) at 77 K before and after loading with ibuprofen. Solid symbols correspond to adsorption plots, and open symbols correspond to desorption plots.

MILs exhibited a Fe−O stretch at 549 cm^{-1}, a carboxylate —C═O stretch at 1602 cm^{-1}, a and −C−O stretch at 1389 cm^{-1}, which are consistent with those previously reported in the literature.[25,28,48] After the structural studies, we optimized drug loading conditions for each material. Considering the polarity of ibuprofen and stability of MILs in organic solvents, we immersed MILs into ibuprofen/hexane solutions with various concentrations for different amounts of time. We found that the best drug loading condition for MIL-88B was 10 mg/mL with a soaking time of 24 h, while for MIL-53, the condition is 30 mg/mL for 72 h with a nanoparticle-to-drug ratio of 1:3. After loading ibuprofen in hexane, the crystal structures of both MIL-88B and MIL-53 were still present (Figure 1), indicating that both materials did not degrade during drug loading procedures. Additionally, ATR-IR studies confirmed that the ibuprofen has been successfully incorporated into both materials, indicated by an increasing intensity of the —C═O stretch by comparison with pure ibuprofen shown in Figure 1b. By analyzing IR and PXRD studies of MIL-88B, we concluded that ibuprofen was successfully incorporated in MIL-88B. However, at this point, we were unclear about whether ibuprofen was adsorbed on the outer surface or encapsulated inside of MIL-53 crystals. Therefore, we applied N_2 gas sorption analysis to monitor the changes in the surface area and available pore sizes of both Fe-MILs after ibuprofen treatments, Figure 3. The specific surface area (SSA) was calculated based on the Brunauer−Emmett−Teller (BET) theory[49] with N_2 sorption isotherms at 77 K (details are available in the Supporting Information). We noticed that the SSA of MIL-53 decreased from 30.1 to 22.1 m^2/g after loading with ibuprofen, indicating that ibuprofen was encapsulated inside of MIL-53 and occupied available channels. A similar trend was also observed for MIL-88B by comparing SSA before and after ibuprofen loading. Table S1 summarizes the surface area changes of both MILs corresponding to drug loading. We also examined the external surface area of both MILs before and after loading with ibuprofen. The *t*-plot studies[50] using Micromeritics software show that the external surface area of ibu-MIL-88B decreased to 21.7 cm^2/g compared to that of pristine MIL-88 of 27.9 cm^2/g. The micropore surface area of MIL-88B decreases from 14.4 to 3.9 cm^2/g after loading with ibuprofen, confirming that majority internal cages were filled with ibuprofen. A similar trend was also noticed on the MIL-53
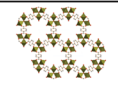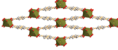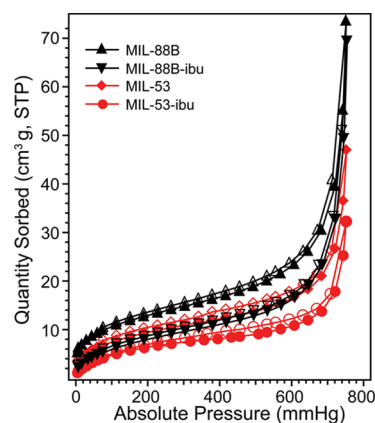
system with a decrease in the external surface area. To eliminate solvent molecules that may interfere with our results, all testing samples were thermally activated in a vacuum oven at 65 °C for over 72 h. Based on their unique crystal structures, the maximum accessible surface areas (theoretical SSA) for MIL-53 and MIL-88B are 2203 m^2/g (H_2 as a probe) and 3042 m^2/g (N_2 as a probe), respectively.[28,51,52] Although the surface areas obtained experimentally are typically smaller than those predicted based on single-crystal structures, this is due to some solvent molecules still remain and a small fraction of framework bonds break, thus block channels during degassing. Furthermore, a strong surface tension can be formed between the adsorbent and adsorbate during the removal of the solvent in vacuum, which may further promote the collapse of channels. The structural loss of porosity affects more for porous crystals with 1D channels, such as MIL-53. Another explanation is attributed to the structural flexibility of iron-based MILs. Unlike their Cr or Al analogues, the channels remain closed for Fe-MIL-53 after the solvent or guest molecule is removed, thus unable nitrogen molecules to enter.[53−55] Scheme S1 illustrates the flexibility of MIL-53 frameworks. Relatively small SSA was also reported for MIL-53 in other studies.[10,28,56] Combining results from PXRD, ATR-IR, and N_2 sorption analyses, we concluded that ibuprofen was successfully encapsulated in MIL-88B and MIL-53.

The driving force for ibuprofen loading is the strong hydrogen-bonding and weak van der Waals interactions between ibuprofen and the hydroxyl groups from the matrix.[10] We also tried a one-pot synthesis method[57] to mix therapeutic agents together with MOF starting materials in a solvothermal setting; however, no desired MIL crystals were formed. We suspect that the carboxylate groups in ibuprofen may compete with terephthalic acid for coordinating with FeO_3 clusters, thus disturbed the formation of MIL-88B and MIL-53. Therefore, we continued with the immersion method for drug loading in this study. To quantify the drug loading capacity of MIL materials, we applied a UV−vis spectrometer to monitor the concentration of ibuprofen at 264 nm (λ_{max}), before and after incorporation into MIL materials. The detailed UV spectra were provided in the Supporting Information. Based on eq 1, the calculated ibuprofen loading amounts approximates 372.2 mg/g of MIL-53 and 194.6 mg/g of MIL-88B, respectively. The drug loading capacities are consistent with previously

reported values.[9,10] Although these values are not as large as the values reported for other MOFs, for example, MIL-101 and MIL-100 (containing much larger volumes because of their rigid structures), both MIL-53 and MIL-88B are significantly better than other porous materials for drug delivery (usually less than 50 mg of drug per gram of the host material, of 5 wt %).[24,58] In our studies, MIL-53 was able to be incorporated about 17% more ibuprofen compared to MIL-88B. We suspected that the higher drug loading capacity observed for MIL-53 is mainly due to the monoclinic symmetry of its structure, facilitating the diffusion of guest molecules. The crystal structures and drug loading capacity for each MIL have been summarized in Table 1. Although Fe-MIL-88B contains a

Table 1. Structures of Fe-Based MIL-88B and MIL-53 and Comparison of Ibuprofen Loading Capacity

Material	Structure[a]	Symmetry	Space Group[b]	Pore Volume ca. (Å³)[c]	Ibuprofen Loading Amount ca. (mg/g)[d]
Fe-MIL-88B		Hexagonal	p-62c	1980	195
Fe-MIL-53		Monoclinic	C2/c	1400	370

[a]Structures are viewed along the c-axis. [b]Space group of dehydrated form.[55,59] [c]Maximum available pore volume with solvent.[10,28] [d]From this study.

larger pore volume than MIL-53, the drug loading capacity is lower than for MIL-53. We presume that the 1D channel of MIL-53 may account for a faster mass transfer of guest molecules compared to the cage-like structure of MIL-88B crystals.

Additionally, we studied the changes in morphology of MIL-88B crystals corresponding to drug loading in hexane. Figure 4 presents the scanning electron microscopy (SEM) images of MIL-88B before and after loading of ibuprofen. MIL-88B exhibited a rice-grain shape with a length of around 500 nm along the c-axis. Larger crystals with a dimension of 2 μm were observed in the same synthesis solution that may attribute to an over-grown crystallization process. After being treated with ibuprofen in hexane, MIL-88B showed no obvious change in morphology, although the population of large crystals has increased. This may indicate a continuous crystal growth of MIL-88B during the drug loading process, which may cause

ibuprofen molecules encapsulated not only within the pores but also trapped inside the particles.

2.2. Drug Elution Studies. After confirming ibuprofen was successfully loaded into both Fe-MILs, we studied the drug elution process of each material. We stirred ibuprofen-loaded MIL-53 and MIL-88B in phosphate buffer saline (PBS), respectively, to mimic drug releasing in a physiologic environment. Solutions were collected in periodic intervals up to 10 days for monitoring ibuprofen elution and degradation of MILs and analyzed using a reversed-phase high-performance liquid chromatography (HPLC). Figure 5
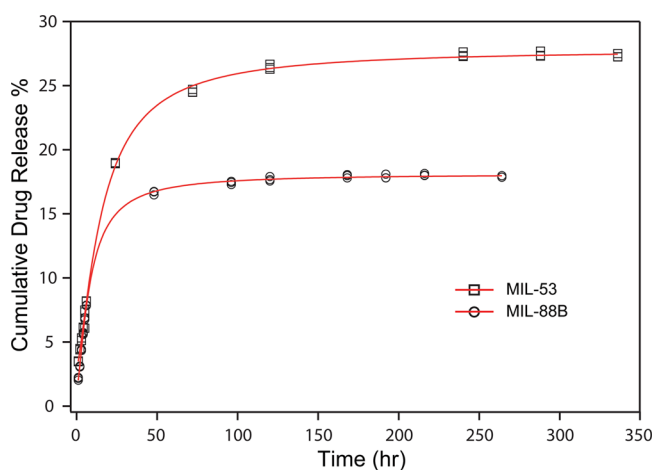

Figure 5. Profiles of cumulative ibuprofen release percentage as a function of soaking time in PBS for MIL-53 (squares) and MIL-88B (circles). The data were fitted with the Hill equation as indicated by the red plots.

displays the cumulative ibuprofen released from treated MIL-53 and MIL-88B as a function of an immersing time. We noticed that the concentration of ibuprofen increased with increasing soaking times for both Fe-MILs, indicating that ibuprofen was released from both materials over time. However, a drug releasing burst was observed for both MILs within the first 24 h, indicating a faster drug elution process, likely due to surface adsorbed species. The drug release profile can be illustrated by two stages: the first stage refers to a fast drug release; the second stage can be treated as a stable phase as the drug concentration increased slightly with respect to the increasing contact time with PBS. A similar two-stage drug
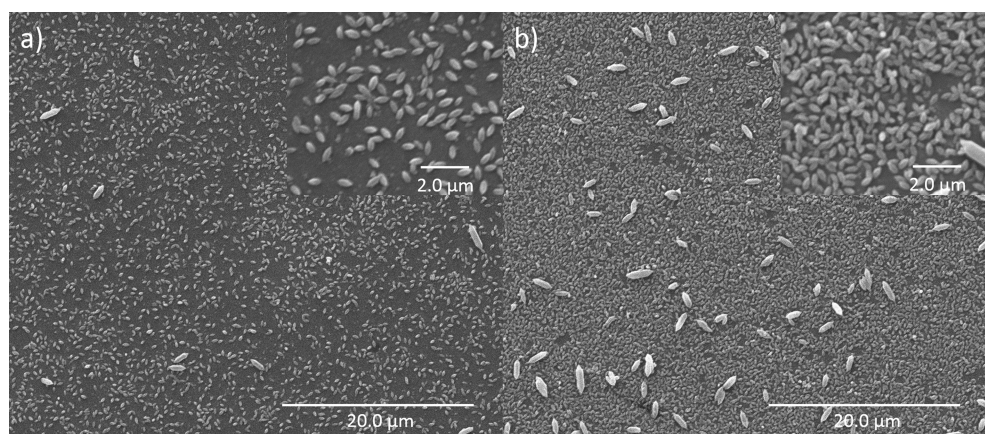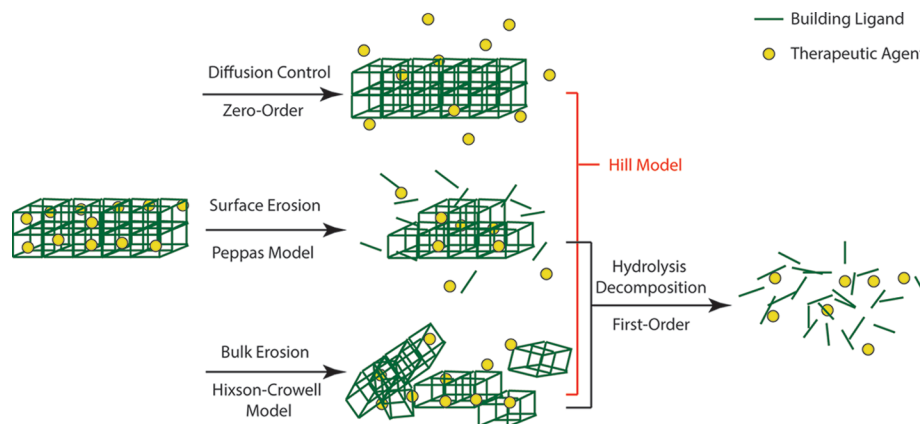

Figure 4. SEM images of MIL-88B crystals (a) before and (b) after ibuprofen loading.

Scheme 1. Illustrative Scheme of Drug Delivery Systems and Models Considered for MIL-88B and MIL-53

release profile was observed previously on Cr-based MIL-53.[10] During our testing period, the accumulative drug releasing amounts were 27.4 and 18.0% for MIL-53 and MIL-88B, respectively. The low drug elution amounts after 10 days indicates that there was still a large amount of ibuprofen that had not been released from the host materials. We think that the low drug releasing amount was due to the slow degradation of Fe-MILs in aqueous. A similar drug elution result was reported by Horcajada et al., showing that Fe-MIL-88B can last up to 21 days in a simulated body fluid.[10] In our study, we noticed that MIL powder was still visible in the testing solution even after 1 month. A slow releasing rate of ibuprofen by MILs after the first two days was similar to the releasing profile of MIL-88B when caffeine was used as the model drug.[60] The slow drug releasing rate is beneficial for drug delivery applications that require drug elution in a controlled manner. Additionally, it is critically important to understand the drug release mechanisms to better adopt MIL materials for drug delivery applications. Therefore, we applied several mathematical models to interpret the drug elution behaviors with consideration of the biodegradable nature of both MILs. Scheme 1 summarizes the drug delivery systems and their fitting models in this work.

The zero-order (eq 2) kinetics is based on Fick's law of diffusion and has been widely used to describe release kinetics for diffusion-controlled reservoir systems, such as nanoparticles and membrane-encapsulated vesicles.[61] Studies show that ibuprofen released by Cr- and Fe-based MIL-53 has followed this model for at least one stage.[10] Considering the biodegradation of both MILs, a first-order kinetic model (eq 3) was used to analyze the drug delivery behaviors. The first-order kinetic equation is based on hydrolysis decomposition behaviors.[35] Moreover, the degradation/erosion of a drug delivery system can be distinguished into two models: surface erosion and bulk erosion. Surface erosion refers to the degradation process, which is mainly restricted to the outermost surface of these porous crystals without harm to the interior. The surface erosion model can be described using the Peppas equation (eq 4).[36,62] The bulk erosion model describes a drug delivery system decomposing into smaller fragments due to material cleavage in physiological environment and can be described by the Hixson−Crowell model (eq 5).[23,37] The Hill model (eq 6) takes into consideration of the limited diffusion and erosion of the matrices.[38] Drug release kinetics is the combined results of drug molecular movement (mass transfer) and host material's behaviors, such as swelling,

degradation, and interactions with guest molecules.[61] Based on the crystal structure and stability of MILs, the higher correlation coefficients were observed in the Hill model for both drug delivery systems, shown in Figure 5, indicating that the ibuprofen release kinetics fits better for a combined model of diffusion, surface, and bulk erosion. The monoclinic structure of MIL-53 is expected to promote the mass transfer of ibuprofen to be released. In comparison, MIL-88B has complex 3D pores, which may reduce the drug releasing rate. Such a controlled drug release profile of MIL-88B is favorable for a desired slow drug delivery process.

Another factor that should be considered is the stability of MILs in aqueous conditions. Most Fe-based MILs are not stable in aqueous environment due to interruption in coordination bonds induced by water molecules. To evaluate the stabilities of MIL-53 and MIL-88B, we monitored the concentration change of the building ligand (terephthalate) for both MILs using HPLC, shown in Figure 6a. We noticed an
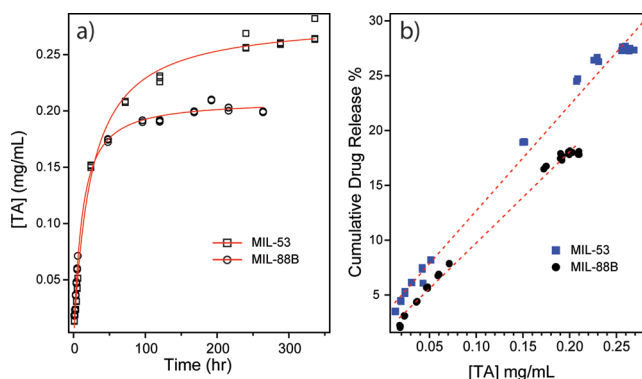

Figure 6. (a) Plots of TA concentration as a function of soaking time in PBS for MIL-53 (open squares) and MIL-88B (open circles). (b) Linear regression correlation between TA concentration change and cumulative drug release percents of both MIL-53 (blue solid squares) and MIL-88B (black solid circles).

increase in the concentration of terephthalate ligands with a longer immersion time in PBS with a similar kinetic profile as the ibuprofen elution process. With the breakdown of frameworks of each MIL, preloaded guest molecules are able to freely diffuse into the surrounding solution. This degradation of MILs can explain the increasing concentrations of ibuprofen even after 10 days. The degradation process also leads to the increase in concentrations of Fe^{3+}, which was

monitored using ICP-AES. This increasing amount of iron is another evidence of MIL decomposition in PBS as a function of time. By performing a linear regression analysis to evaluate the relationship between drug release and material degradation, a linear relationship was observed for both systems (Figure 6b), indicating that material degradation has caused the drug elution. We believe that the drug releasing process is a combination of ibuprofen desorption/diffusion and, more importantly, MIL material degradation. Based on the releasing profiles, we believe that the degradation of carrier matrices is the dominant factor on drug releasing.

2.3. Cytotoxicity Studies. The chemical composition of MIL-88B (iron and terephthalate) was one of the factors why MIL-88B was selected as a carrier for drug delivery applications. The toxicity of Fe-based MOFs is low when compared to Zr-based MOFs that exhibit better stability in aqueous conditions. In addition, Fe-based MOF nanoparticles are also classified as safe for the delivery of contrast agents.[25] We have tested the cytotoxicity of MIL-88B nanoparticles because its monotonic release profile of ibuprofen (Figure 5) seems more suitable for drug delivery applications than MIL-53.

We evaluated the cytotoxicity of the MIL-88B with the NIH-3T3 Swiss mouse fibroblast cells by adding the particles to the media (after sterilization). After 48 h incubation, the CellTiter96 viability assay (Figure 7) shows that the particles
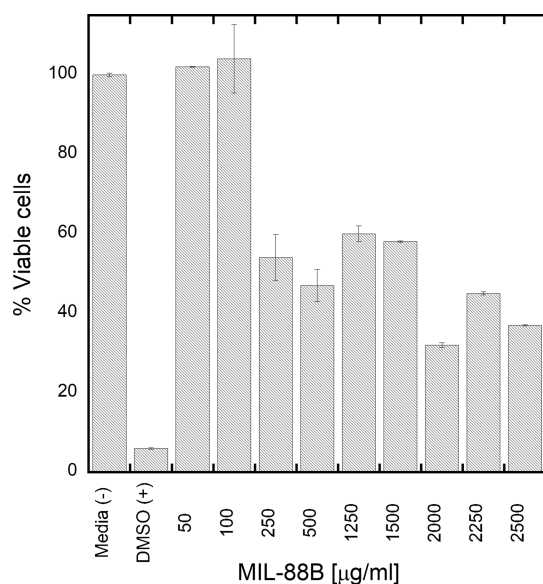

Figure 7. Effect of MIL-88B on viability of NIH-3T3 Swiss mouse fibroblasts. The error bar represents a standard deviation from 18 independent measurements.

have no adverse effect on cell viability up to 0.1 mg/mL. After the addition of 0.25 mg/mL, the viability decreases to about 60% and then drops to about 40% after increasing the concentration to 2 mg/mL. The cell viability did not drop below 40% for the maximum tested concentration of 2.5 mg/mL.

The cellular uptake of nanoparticles strongly depends on their size and surface groups and, in this case, also the MOF composition. Both metal ion and organic ligand can contribute to toxicity. In Figure 4, the size and shape of the studied MIL-88B show that the majority of the material is formed as approximately 500 nm (along the *c*-axis) rice-grain shaped

particles. Thus, the nanoparticles are significantly larger than previously tested MIL-88B by Tamames-Tabar et al.[25] where the average size of nanoparticle was 100 ± 20 nm. The reported toxicity at 50% was 1.26 mg/mL recorded in HeLa cells and 0.37 mg/mL recorded in J774 cells. The differences were attributed to the different phagocytic pathways in tested cell lines since J774 is a macrophage cell line prone to increased phagocytosis. In the case of our studies, the toxicity of the MIL-88B measured with 3T3 cells is lower than in both previously studied cell lines. Both HeLa and 3T3 cells are not macrophages, so the difference in toxicity is most likely related to the larger particle size in our studies. At this point, we cannot conclude with certainty what is the main mechanism of lower toxicity of MIL-88 in our study compered to Tamames-Tabar et al.,[25] but we can identify two sources of this behavior. Either the large size of the nanoparticles decreases the cellular uptake or the larger size of nanoparticles slows down the decomposition of individual nanoparticles within the cell and, thus, lowers the toxicity of the tested material.

3. CONCLUSIONS

In all, two types of Fe-MOFs, MIL-88B and MIL-53, were evaluated for drug loading and elution with ibuprofen as a model drug. We concluded that the monoclinic crystal structure of MIL-53 promotes a high drug loading capacity due to a favorable mass transfer within the 1D channels, but the same structure also exhibits a faster and higher drug release profile. MIL-88B with a 3D cage structure offers more flexibility and better control over drug elution behavior. These structural differences between Fe-MOFs that are formed with identical SBUs and ligands strongly suggest that directing crystal structure can tune drug elution behavior. In addition, we show that the MIL-88B in the form of large nanoparticles is biodegradable and noncytotoxic. We believe that the ability to direct structures of Fe-MOFs together with its high biocompatibility will allow in the future to create the "designer" structures for the delivery of particular drug with desired release profile.

4. EXPERIMENTAL SECTION

4.1. Materials. All chemicals were reagent grade or better and used as received, included: iron(III) chloride (hexahydrate, 99 + %, Acros), terephthalic acid (TA, 99 + %, Acros), *N,N*-dimethylformamide (Fisher Chemical, ACS Certified), sodium hydroxide (2.0 N Standardized Solution, Alfa Aesar), hexanes (Fisher Chemical, ACS Certified), ibuprofen (99%, Acros), phosphate-buffered saline (PBS, pH = 7.2, 1×, Gibco), trifluoroacetic acid (HPLC Grade, Acros), Milli-Q water (18 MΩ· cm, Millipore), and acetonitrile (HPLC Grade, Fisher Chemical).

4.2. Synthesis of MIL-53. Fe-MIL-53 was synthesized according to the literature.[10] TA (0.7 mmol) and $FeCl_3 \cdot 6H_2O$ (0.7 mmol) were dissolved in 15 mL of DMF in a glass reactor. To obtain a sufficient material, six reactors were prepared together. The mixed solution was placed in a preheated oven at 150 °C for 15 h to form Fe-MIL-53 crystals. After cooling to room temperature, the crystals were separated by vacuum filtration and rinsed with DMF, acetone, and deionized water. After that, the crystals were vacuum dried at room temperature and followed by drying in a gravity oven at 110 °C to remove extra moisture. These crystals were named as-synthesized MIL-53 and were performed PXRD analysis. Solvent exchange for

trapped DMF for water by stirring as-synthesized MIL-53 in deionized water for 24 h. The MIL-53 colloid was then centrifuged at 5000 rpm (Eppendorf, Centrifuge 5430). For the removal of water and free up porous space for drug loading, MIL-53 crystals were further dried in a vacuum oven (Fisher Scientific, Isotemp vacuum oven model 281A) at 65 °C for 24 h.

4.3. Synthesis of MIL-88B. Fe-MIL-88B crystals were synthesized via a revised solvothermal method according to a previous reported procedure.[9] FeCl$_3$·6H$_2$O (1 mmol) and TA (1 mmol) were dispersed in 5 mL of DMF with 0.4 mL of sodium hydroxide (2.0 N) in a glass reactor. The mixed solution was sonicated for 3 min before being placed in a preheated oven at 100 °C for 12 h. After the solvothermal synthesis, the orange solid, Fe-MIL-88B, was recovered by filtration and washed with DMF, deionized water, and acetone. The product was then placed in a gravity oven at 110 °C for 24 h to completely dry as-synthesized Fe-MIL-88B.

To make sure the MIL-88B structure was clear from DMF and unreacted ligands, additional solvent exchange procedures were performed: MIL-88B was stirred in deionized water for 24 h, solids were then collected by vacuum filtration, and washed with deionized water three times. Finally, the crystals were dried in a vacuum oven at 65 °C for 24 h.

4.4. Drug Loading Studies. Dry Fe-MIL crystals were stirred in ibuprofen/hexane solutions with varying concentrations for different set amount of times. The material-to-ibuprofen mass ratio was kept at 1:3. We found that the best ibuprofen loading condition for MIL-53 was stirring 50 mg of MIL-53 with 5 mL of ibuprofen/hexane solution (30 mg/mL) for 72 h. The optimal ibuprofen loading condition for MIL-88B was 20 mg of MIL-88 mixed with 6 mL of ibuprofen/hexane (10 mg/mL) for 24 h. After desired soaking period, the drug encapsulated crystals were collected by centrifugation at 5000 rpm for 20 min. The supernatant was saved for UV analysis for drug loading quantification. The precipitate (Fe-MILs loaded with ibuprofen) was dried in a vacuum oven at 65 °C for 24 h. The drug loading capacity (LC, mg of ibuprofen per gram of material) of each Fe-MIL was evaluated based on the following equation

$$LC = \frac{(C_0 - C_t) \times V}{m} \tag{1}$$

where C_0 is the initial ibuprofen concentration, C_t is the ibuprofen concentration at time t, V is the total volume of ibuprofen solution, and m is the mass of Fe-MIL applied in the mixture solution.

4.5. Drug Elution Studies. An amount of 10 mg of dry ibuprofen encapsulated MILs was soaked and stirred in 40 mL of PBS at room temperature for drug release studies. A 2 mL aliquot of mixed solution was collected at each hour for the first 6 h, one sample was then collected each day for the next ten days. The collected solution was filtered through a syringe filter (PVDF, 0.45 μm, 13 mm diameter) to remove large Fe-MIL solids before analysis. Ibuprofen release amounts and Fe-MIL degradation rates were examined by monitoring the changes in concentrations of ibuprofen and TA over time using a reversed-phase HPLC. Horcajada et al. reported a two-stage drug release profile for MIL-53 materials.[10] In this study, we observed a similar trend on both Fe-based MIL-53 and MIL-88B systems. The release kinetics of each system on both stages was evaluated using different drug delivery models, including zero-order, first-order, Peppas, Hixson−Crowell, and

Hill models. If a higher correlation coefficient is observed, it confirms that the drug delivery system follows the corresponding kinetic model.

A zero-order drug delivery model is commonly used to describe the diffusion behaviors of a system and can be expressed in the following equation[34]

$$\frac{M_t}{M_\infty} = kt \tag{2}$$

where, M_t and M_∞ represent the absolute cumulative amount of released drug at the time t and at infinite time, and k is the release rate constant. The ratio of M_t and M_∞ represents the cumulative drug release percent.

The first-order kinetic equation takes consideration of material degradation in water and can be expressed as followed[35]

$$\ln\left(1 - \frac{M_t}{M_\infty}\right) = -kt \tag{3}$$

The Peppas model was first proposed in 1985[36] and is now widely used for modeling polymer-based drug delivery systems with surface erosion. It can be expressed as the following equation where n is the release exponent

$$\frac{M_t}{M_\infty} = kt^n \tag{4}$$

We also applied the Hixson−Crowell model to consider a bulk-erosion system since Fe-MILs may degrade into smaller crystals in physiological environment. The Hixson−Crowell model can be expressed as follows[37]

$$\sqrt[3]{\left(1 - \frac{M_t}{M_\infty}\right)} = -kt \tag{5}$$

The Hill model was also applied to fit the cumulative drug release percent as a function of time. This model takes consideration of diffusion and degradation processes of the matrices and can be expresses as follows[38]

$$\frac{M_t}{M_\infty} = M_0 + (M_{Eq} - M_0)/\left[1 + \left(\frac{t_{1/2}}{t}\right)^k\right] \tag{6}$$

where M_0 and M_{Eq} represent the drug release amounts at time zero and at an equilibrium condition, and $t_{1/2}$ represents the time when the slope of the cumulative drug release curve has the highest value.

4.6. Cytotoxicity Studies. A CellTiter 96 nonradioactive cell proliferation assay (MTT) from Promega was used to evaluate the cytotoxicity of MIL-88B with the NIH-3T3 Swiss mouse fibroblasts (ATCC) cell line. Cells were cultured in complete (10% fetal bovine serum, 1% penicillin streptomycin-glutamine) Dulbecco's modified Eagle medium (DMEM) and incubated at 37 °C in a humidified 5% CO$_2$ atmosphere until 90% confluent. Sterile MIL-88B (3.5 mg) was dissolved in DMEM through sonication to serve as stock solution. PBS and trypsin were used to induce detachment of 3T3 cells. In a 96-well plate, cells were seeded at a density of 1.0×10^4 cells/well. Concentrations (0.05−2.5 mg/mL) of the stock solution were then added to the plate and incubated for 48 h. Subsequently, the CellTiter 96 assay was performed. The plate reader (Thermo Scientific Varioskan Flash Reader) was used to

record absorption at 570 nm. Each point was calculated from 18 repeats: 6 wells, 3 plates.

4.7. Characterization. Powder X-ray diffraction (PXRD) measurements were carried out on a SmartLab X-Ray diffractometer (Rigaku). Bragg–Brentano Focusing measurements were conducted using a Cu Kα_1 (λ = 1.5406 Å) radiation source. The diffraction angles of measurement were between 7 and 20 degrees with steps of 0.008 degrees.

Infrared spectroscopic studies were performed on a Bruker Alpha I attenuated total reflectance infrared (ATR-IR) spectrometer. All spectra were collected in the range of 4000–400 cm^{-1} at a resolution of 4 cm^{-1} with 64 scans per spectrum.

N$_2$ sorption studies of Fe-MILs before and after ibuprofen loading were performed on a Micromeritics 2020PLUS surface characterization analyzer at 77 K using liquid nitrogen. Prior to measurements, approximately 50 mg of sample was degassed under vacuum at 60 °C for over 12 h. The sample tube was immersed in a liquid nitrogen dewar during measurements. The gas adsorption isotherms were collected as a function of pressure up to 800 torr.

Scanning electron microscopy (SEM, FEI Quanta 650) was applied to study the morphology changes of MIL-88B crystals before and after drug loading. The images were taken with an acceleration voltage of 20 kV and a working distance of 9.4 mm in a high vacuum condition. Gold-coated silicon substrates were coated with desired MIL crystal samples by a dip-coater (Chemat Technology). For increased resolution, all samples were sputter-coated with gold prior to SEM imaging.

A UV–vis spectrophotometer (Shimadzu, UV-1700) was applied to measure ibuprofen loading amounts by monitoring the wavelength at 264 nm (λ_{max} for ibuprofen in hexane). A standard curve of ibuprofen in hexane was created based on a concentration range of 0.001–0.025 mg/mL. The absorbance of ibuprofen before and after drug loading was measured in triplicate with hexane as the blank. For solutions with concentrations out of range of the standard curve, samples were diluted with hexane before measurements.

High-performance liquid chromatography (HPLC, Thermo Scientific, Ultimate 3000) was employed to study drug release kinetics. A reverse-phase C18 analytical column (Agilent, Zorbax 300SB-C18, 4.6 x 250 mm 5-μm) was used along with the mobile phase of water and acetonitrile (50:50 v/v) with 0.08% trifluoroacetic acid in each solvent with a pump rate of 1.5 mL/min. The UV detector was set at wavelengths of 215 and 242 nm at room temperature. A sample volume of 20 μL was injected, and all analyses were performed in triplicate. Standard calibration curves of ibuprofen and TA in PBS were created separately by plotting retention time peak area (mV × s) versus concentration. The peak of ibuprofen was observed at a retention time of 5.2 min in a UV channel of 215 nm. The peak of TA showed up at 1.9 min in the channel of 242 nm.

ASSOCIATED CONTENT

Ⓢ Supporting Information

The Supporting Information is available free of charge at https://pubs.acs.org/doi/10.1021/acsomega.9b03696.

UV–vis spectra, BET plots and parameters, and drug release models (PDF)

AUTHOR INFORMATION

Corresponding Author

Fangyuan Tian − *Department of Chemistry and Biochemistry, California State University Long Beach, Long Beach, California 90840, United States;* ⓞ orcid.org/0000-0003-4141-7286; Phone: 1-(562)-985-2115; Email: fangyuan.tian@csulb.edu; Fax: 1-(562)-985-8557

Authors

Hao Pham − *Department of Physical Sciences, Long Beach City College, Long Beach, California 90808, United States*

Kimberly Ramos − *Chemistry Department, Cerritos College, Norwalk, California 90650, United States*

Andy Sua − *Department of Chemistry and Biochemistry, California State University Long Beach, Long Beach, California 90840, United States*

Jessica Acuna − *Department of Chemistry and Biochemistry, California State University Long Beach, Long Beach, California 90840, United States*

Katarzyna Slowinska − *Department of Chemistry and Biochemistry, California State University Long Beach, Long Beach, California 90840, United States;* ⓞ orcid.org/0000-0001-6468-2918

Travis Nguyen − *Department of Chemistry and Biochemistry, California State University Long Beach, Long Beach, California 90840, United States*

Angela Bui − *Department of Chemistry and Biochemistry, California State University Long Beach, Long Beach, California 90840, United States*

Mark D. R. Weber − *Department of Chemistry and Biochemistry, California State University Long Beach, Long Beach, California 90840, United States*

Complete contact information is available at:
https://pubs.acs.org/10.1021/acsomega.9b03696

Author Contributions

All authors have given approval to the final version of the manuscript.

Notes

The authors declare no competing financial interest.

REFERENCES

(1) Zelikin, A. N.; Ehrhardt, C.; Healy, A. M. Materials and Methods for Delivery of Biological Drugs. *Nat. Chem.* **2016**, *8*, 997−1007.

(2) Enlow, E. M.; Luft, J. C.; Napier, M. E.; DeSimone, J. M. Potent Engineered PLGA Nanoparticles by Virtue of Exceptionally High Chemotherapeutic Loadings. *Nano Lett.* **2011**, *11*, 808–813.

(3) Zhu, L.; Li, M.; Liu, X.; Jin, Y. Drug-Loaded PLGA Electrospraying Porous Microspheres for the Local Therapy of Primary Lung Cancer via Pulmonary Delivery. *ACS Omega* **2017**, *2*, 2273–2279.

(4) Wang, J.; Kumeria, T.; Bezem, M. T.; Wang, J.; Sailor, M. J. Self-Reporting Photoluminescent Porous Silicon Microparticles for Drug Delivery. *ACS Appl. Mater. Interfaces* **2018**, *10*, 3200–3209.

(5) Singh, N.; Karambelkar, A.; Gu, L.; Lin, K.; Miller, J. S.; Chen, C. S.; Sailor, M. J.; Bhatia, S. N. Bioresponsive Mesoporous Silica Nanoparticles for Triggered Drug Release. *J. Am. Chem. Soc.* **2011**, *133*, 19582–19585.

(6) Tavolaro, A.; Riccio, I. I.; Tavolaro, P. Hydrothermal Synthesis of Zeolite Composite Membranes and Crystals as Potential Vectors for Drug-Delivering Biomaterials. *Microporous Mesoporous Mater.* **2013**, *167*, 62–70.

(7) Huxford, R. C.; Della Rocca, J.; Lin, W. Metal–organic Frameworks as Potential Drug Carriers. *Curr. Opin. Chem. Biol.* **2010**, *14*, 262–268.

(8) Rojas, S.; Colinet, I.; Cunha, D.; Hidalgo, T.; Salles, F.; Serre, C.; Guillou, N.; Horcajada, P. Toward Understanding Drug Incorporation and Delivery from Biocompatible Metal–organic Frameworks in View of Cutaneous Administration. *ACS Omega* **2018**, *3*, 2994–3003.

(9) Horcajada, P.; Chalati, T.; Serre, C.; Gillet, B.; Sebrie, C.; Baati, T.; Eubank, J. F.; Heurtaux, D.; Clayette, P.; Kreuz, C.; et al. Porous Metal-organic-Framework Nanoscale Carriers as a Potential Platform for Drug Delivery and Imaging. *Nat. Mater.* **2010**, *9*, 172–178.

(10) Horcajada, P.; Serre, C.; Maurin, G.; Ramsahye, N. A.; Balas, F.; Vallet-Regí, M.; Sebban, M.; Taulelle, F.; Férey, G. Flexible Porous Metal-organic Frameworks for a Controlled Drug Delivery. *J. Am. Chem. Soc.* **2008**, *130*, 6774–6780.

(11) Miller, S. R.; Heurtaux, D.; Baati, T.; Horcajada, P.; Grenèche, J.-M.; Serre, C. Biodegradable Therapeutic MOFs for the Delivery of Bioactive Molecules. *Chem. Commun.* **2010**, *46*, 4526–4528.

(12) Eddaoudi, M.; Moler, D. B.; Li, H.; Chen, B.; Reineke, T. M.; O'Keeffe, M.; Yaghi, O. M. Modular Chemistry: Secondary Building Units as a Basis for the Design of Highly Porous and Robust Metal–organic Carboxylate Frameworks. *Acc. Chem. Res.* **2001**, *34*, 319–330.

(13) Ruiz, M. A.; Sua, A.; Tian, F. Covalent Attachment of Metal-organic Framework Thin Films on Surfaces. In *Encyclopedia of Interfacial Chemistry: Surface Science and Electrochemistry*; Elsevier: 2018; Vol. *4*, pp 646–671.

(14) Li, J.-R.; Kuppler, R. J.; Zhou, H.-C. Selective Gas Adsorption and Separation in Metal-organic Frameworks. *Chem. Soc. Rev.* **2009**, *38*, 1477–1504.

(15) Farrusseng, D.; Aguado, S.; Pinel, C. Metal-organic Frameworks: Opportunities for Catalysis. *Angew. Chem., Int. Ed.* **2009**, *48*, 7502–7513.

(16) Kuo, C.-H.; Tang, Y.; Chou, L.-Y.; Sneed, B. T.; Brodsky, C. N.; Zhao, Z.; Tsung, C.-K. Yolk-Shell Nanocrystal@ZIF-8 Nanostructures for Gas-Phase Heterogeneous Catalysis with Selectivity Control. *J. Am. Chem. Soc.* **2012**, *134*, 14345–14348.

(17) Yang, J.; Zhang, F.; Lu, H.; Hong, X.; Jiang, H.; Wu, Y.; Li, Y. Hollow Zn/Co ZIF Particles Derived from Core-Shell ZIF-67@ZIF-8 as Selective Catalyst for the Semi-Hydrogenation of Acetylene. *Angew. Chem., Int. Ed.* **2015**, *127*, 11039–11043.

(18) Dhakshinamoorthy, A.; Alvaro, M.; Garcia, H. Commercial Metal-organic Frameworks as Heterogeneous Catalysts. *Chem. Commun.* **2012**, *48*, 11275–11288.

(19) Giménez-Marqués, M.; Hidalgo, T.; Serre, C.; Horcajada, P. Nanostructured Metal–organic Frameworks and Their Bio-Related Applications. *Coord. Chem. Rev.* **2016**, *307*, 342–360.

(20) Gaudin, C.; Cunha, D.; Ivanoff, E.; Horcajada, P.; Chevé, G.; Yasri, A.; Loget, O.; Serre, C.; Maurin, G. A Quantitative Structure Activity Relationship Approach to Probe the Influence of the Functionalization on the Drug Encapsulation of Porous Metal-organic Frameworks. *Microporous Mesoporous Mater.* **2012**, *157*, 124–130.

(21) Wu, M.-X.; Yang, Y.-W. Metal-organic Framework (MOF)-Based Drug/Cargo Delivery and Cancer Therapy. *Adv. Mater.* **2017**, *29*, 1606134.

(22) Keskin, S.; Kızılel, S. Biomedical Applications of Metal organic Frameworks. *Ind. Eng. Chem. Res.* **2011**, *50*, 1799–1812.

(23) Huang, W.; Tsui, C. P.; Tang, C. Y.; Gu, L. Effects of Compositional Tailoring on Drug Delivery Behaviours of Silica Xerogel/Polymer Core-Shell Composite Nanoparticles. *Sci. Rep.* **2018**, *8*, 13002.

(24) Cullis, P. R.; Mayer, L. D.; Bally, M. B.; Madden, T. D.; Hope, M. J. Generating and Loading of Liposomal Systems for Drug-Delivery Applications. *Adv. Drug Delivery Rev.* **1989**, *3*, 267–282.

(25) Tamames-Tabar, C.; Cunha, D.; Imbuluzqueta, E.; Ragon, F.; Serre, C.; Blanco-Prieto, M. J.; Horcajada, P. Cytotoxicity of Nanoscaled Metal–organic Frameworks. *J. Mater. Chem. B* **2014**, *2*, 262–271.

(26) Filippousi, M.; Turner, S.; Leus, K.; Siafaka, P. I.; Tseligka, E. D.; Vandichel, M.; Nanaki, S. G.; Vizirianakis, I. S.; Bikiaris, D. N.; Van Der Voort, P.; et al. Biocompatible Zr-Based Nanoscale MOFs Coated with Modified Poly(ε-Caprolactone) as Anticancer Drug Carriers. *Int. J. Pharm.* **2016**, *509*, 208–218.

(27) Al Haydar, M.; Abid, H.; Sunderland, B.; Wang, S. Metal organic Frameworks as a Drug Delivery System for Flurbiprofen. *Drug Des., Dev. Ther.* **2017**, *Volume 11*, 2685–2695.

(28) Horcajada, P.; Salles, F.; Wuttke, S.; Devic, T.; Heurtaux, D.; Maurin, G.; Vimont, A.; Daturi, M.; David, O.; Magnier, E.; et al. How Linker's Modification Controls Swelling Properties of Highly Flexible Iron(III) Dicarboxylates MIL-88. *J. Am. Chem. Soc.* **2011**, *133*, 17839–17847.

(29) Serre, C.; Surblé, S.; Mellot-Draznieks, C.; Filinchuk, Y.; Férey, G. Evidence of Flexibility in the Nanoporous Iron(Iii) Carboxylate MIL-89. *Dalton Trans.* **2008**, *0*, 5462.

(30) Surblé, S.; Serre, C.; Mellot-Draznieks, C.; Millange, F.; Férey, G. A New Isoreticular Class of Metal-organic-Frameworks with the MIL-88 Topology. *Chem. Commun.* **2006**, *3*, 284–286.

(31) McKinlay, A. C.; Morris, R. E.; Horcajada, P.; Férey, G.; Gref, R.; Couvreur, P.; Serre, C. BioMOFs: Metal-organic Frameworks for Biological and Medical Applications. *Angew. Chem. Int. Ed.* **2010**, *49*, 6260–6266.

(32) Scherb, C.; Schödel, A.; Bein, T. Directing the Structure of Metal-organic Frameworks by Oriented Surface Growth on an organic Monolayer. *Angew. Chem. Int.* **2008**, *47*, 5777–5779.

(33) Whitfield, T. R.; Wang, X.; Liu, L.; Jacobson, A. J. Metal-organic Frameworks Based on Iron Oxide Octahedral Chains Connected by Benzenedicarboxylate Dianions. *Solid State Sci.* **2005**, *7*, 1096–1103.

(34) Huang, X.; Brazel, C. S. On the Importance and Mechanisms of Burst Release in Matrix-Controlled Drug Delivery Systems. *J. Controlled Release* **2001**, *73*, 121–136.

(35) Körber, M. PLGA Erosion: Solubility- or Diffusion-Controlled? *Pharm. Res.* **2010**, *27*, 2414–2420.

(36) Peppas, N. A. Analysis of Fickian and Non-Fickian Drug Release from Polymers. *Pharm. Acta Helv.* **1985**, *60*, 110–111.

(37) Costa, P.; Sousa Lobo, J. M. Modeling and Comparison of Dissolution Profiles. *Eur. J. Pharm. Sci.* **2001**, *13*, 123–133.

(38) Goutelle, S.; Maurin, M.; Rougier, F.; Barbaut, X.; Bourguignon, L.; Ducher, M.; Maire, P. The Hill Equation: A Review of Its Capabilities in Pharmacological Modelling. *Fundam. Clin. Pharmacol.* **2008**, *22*, 633–648.

(39) Xu, B.; Yang, H.; Cai, Y.; Yang, H.; Li, C. Preparation and Photocatalytic Property of Spindle-like MIL-88B(Fe) Nanoparticles. *Inorg. Chem. Commun.* **2016**, *67*, 29–31.

(40) Shi, L.; Wang, T.; Zhang, H.; Chang, K.; Meng, X.; Liu, H.; Ye, J. An Amine-Functionalized Iron(III) Metal-organic Framework as Efficient Visible-Light Photocatalyst for Cr(VI) Reduction. *Adv. Sci.* **2015**, *2*, 1500006.

(41) Bragg, W. L. The Diffraction of Short Electromagnetic Waves by a Crystal. *Proc. Camb. Philol. Soc.* **1913**, *17*, 43−57.

(42) Loiseau, T.; Serre, C.; Huguenard, C.; Fink, G.; Taulelle, F.; Henry, M.; Bataille, T.; Férey, G. A Rationale for the Large Breathing of the Porous Aluminum Terephthalate (MIL-53) upon Hydration. *Chemistry* **2004**, *10*, 1373−1382.

(43) Ma, M.; Noei, H.; Mienert, B.; Niesel, J.; Bill, E.; Muhler, M.; Fischer, R. A.; Wang, Y.; Schatzschneider, U.; Metzler-Nolte, N. Iron Metal-organic Frameworks MIL-88B and NH$_2$-MIL-88B for the Loading and Delivery of the Gasotransmitter Carbon Monoxide. *Chem. - A Eur. J.* **2013**, *19*, 6785−6790.

(44) Walton, R. I.; Munn, A. S.; Guillou, N.; Millange, F. Uptake of Liquid Alcohols by the Flexible Fe^{III} Metal-organic Framework MIL-53 Observed by Time-Resolved In Situ X-Ray Diffraction. *Chem. - A Eur. J.* **2011**, *17*, 7069−7079.

(45) Nikseresht, A.; Daniyali, A.; Ali-Mohammadi, M.; Afzalinia, A.; Mirzaie, A. Ultrasound-Assisted Biodiesel Production by a Novel Composite of Fe(III)-Based MOF and Phosphotangestic Acid as Efficient and Reusable Catalyst. *Ultrason. Sonochem.* **2017**, *37*, 203−207.

(46) Feng, X.; Chen, H.; Jiang, F. In-Situ Ethylenediamine-Assisted Synthesis of a Magnetic Iron-Based Metal-organic Framework MIL-53(Fe) for Visible Light Photocatalysis. *J. Colloid Interface Sci.* **2017**, *494*, 32−37.

(47) Alsop, R. J.; Armstrong, C. L.; Maqbool, A.; Toppozini, L.; Dies, H.; Rheinstädter, M. C. Cholesterol Expels Ibuprofen from the Hydrophobic Membrane Core and Stabilizes Lamellar Phases in Lipid Membranes Containing Ibuprofen. *Soft Matter* **2015**, *11*, 4756−4767.

(48) Wang, Y.; Muramatsu, A.; Sugimoto, T. FTIR Analysis of Well-Defined α-Fe$_2$O$_3$ Particles. *Colloids Surf., A* **1998**, *134*, 281−297.

(49) Brunauer, S.; Emmett, P. H.; Teller, E. Adsorption of Gases in Multimolecular Layers. *J. Am. Chem. Soc.* **1938**, *60*, 309−319.

(50) Harkins, W. D.; Jura, G. An Adsorption Method for the Determination of the Area of a Solid without the Assumption of a Molecular Area, and the Area Occupied by Nitrogen Molecules on the Surfaces of Solids. *J. Chem. Phys.* **1943**, *11*, 431−432.

(51) Düren, T.; Millange, F.; Férey, G.; Walton, K. S.; Snurr, R. Q. Calculating Geometric Surface Areas as a Characterization Tool for Metal - organic Frameworks. *J. Phys. Chem. C* **2007**, *111*, 15350−15356.

(52) First, E. L.; Floudas, C. A. MOFomics: Computational Pore Characterization of Metal-organic Frameworks. *Microporous Mesoporous Mater.* **2013**, *165*, 32−39.

(53) Vu, T. A.; Le, G. H.; Dao, C. D.; Dang, L. Q.; Nguyen, K. T.; Nguyen, Q. K.; Dang, P. T.; Tran, H. T. K.; Duong, Q. T.; Nguyen, T. V.; et al. Arsenic Removal from Aqueous Solutions by Adsorption Using Novel MIL-53(Fe) as a Highly Efficient Adsorbent. *RSC Adv.* **2015**, *5*, 5261−5268.

(54) Millange, F.; Guillou, N.; Walton, R. I.; Grenèche, J.-M.; Margiolaki, I.; Férey, G. Effect of the Nature of the Metal on the Breathing Steps in MOFs with Dynamic Frameworks. *Chem. Commun.* **2008**, *39*, 4732−4734.

(55) Devic, T.; Horcajada, P.; Serre, C.; Salles, F.; Maurin, G.; Moulin, B.; Heurtaux, D.; Clet, G.; Vimont, A.; Grenéche, J.-M.; et al. Functionalization in Flexible Porous Solids: Effects on the Pore Opening and the Host-Guest Interactions. *J. Am. Chem. Soc.* **2010**, *132*, 1127−1136.

(56) Matsuyama, K.; Hayashi, N.; Yokomizo, M.; Kato, T.; Ohara, K.; Okuyama, T. Supercritical Carbon Dioxide-Assisted Drug Loading and Release from Biocompatible Porous Metal-organic Frameworks. *J. Mater. Chem. B* **2014**, *2*, 7551−7558.

(57) Zheng, H.; Zhang, Y.; Liu, L.; Wan, W.; Guo, P.; Nyström, A. M.; Zou, X. One-Pot Synthesis of Metal-organic Frameworks with Encapsulated Target Molecules and Their Applications for Controlled Drug Delivery. *J. Am. Chem. Soc.* **2016**, *138*, 962−968.

(58) Spokoyny, A. M.; Kim, D.; Sumrein, A.; Mirkin, C. A. Infinite Coordination Polymer Nano- and Microparticle Structures. *Chem. Soc. Rev.* **2009**, *38*, 1218.

(59) Serre, C.; Mellot-Draznieks, C.; Surblé, S.; Audebrand, N.; Filinchuk, Y.; Férey, G. Role of Solvent-Host Interactions That Lead to Very Large Swelling of Hybrid Frameworks. *Science* **2007**, *315*, 1828−1831.

(60) Liédana, N.; Galve, A.; Rubio, C.; Téllez, C.; Coronas, J. CAF@ZIF-8: One-Step Encapsulation of Caffeine in MOF. *ACS Appl. Mater. Interfaces* **2012**, *4*, 5016−5021.

(61) Siepmann, J.; Siepmann, F. Mathematical Modeling of Drug Delivery. *Int. J. Pharm.* **2008**, *364*, 328−343.

(62) Rothstein, S. N.; Federspiel, W. J.; Little, S. R. A Unified Mathematical Model for the Prediction of Controlled Release from Surface and Bulk Eroding Polymer Matrices. *Biomaterials* **2009**, *30*, 1657−1664.